Article

Effect of Isomerization and Copolymerization of Itaconic Anhydride During the Synthesis of Renewable Monomers Using Vegetable Oils

Caroline Gaglieri, [a] *Rafael T. Alarcon,* [b] *Aniele de Moura,* [a] *Raquel Magri,* [a] *Daniel Rinaldo* [a,c] *and Gilbert Bannach* *,[a]

aLaboratório de Materiais Poliméricos, Faculdade de Ciências, Departamento de Química, Universidade Estadual Paulista Júlio de Mesquita Filho (Unesp), 17033-260 Bauru-SP, Brazil

bLaboratório de Análise Térmica, Eletroanalítica e Química de Soluções (LATEQS), Instituto de Química de São Carlos (IQSC), Universidade de São Paulo (USP), 13566-590 São Carlos-SP, Brazil

cInstituto de Estudos Avançados do Mar (IEAMAR), Universidade Estadual Paulista Júlio de Mesquita Filho (Unesp), 11350-011 São Vicente-SP, Brazil

Vegetable oils are alternatives to producing renewable monomers since they are biomass. It is possible to react them with anhydrides by heating to provide monomers with high reactivity. However, after the reaction of grape seed oil with itaconic anhydride, it was observed the occurrence of parallel reactions that had not been observed when the same oil was reacted with maleic anhydride. Some articles in the literature have reported that temperature and bases can isomerize itaconic anhydride into citraconic anhydride, which is more stable at room temperature. However, they have not focused on completely understanding how this phenomenon occurred nor studied it in processes that involve microwave irradiation. Therefore, this paper presents a complete characterization and investigation about the thermal behavior of itaconic anhydride and how it can affect the monomer synthesis performed under heating.

Keywords: biomass, citraconic anhydride, itaconic anhydride, grape seed oil, thermal copolymerization, solvent effect

Introduction

Due to the increase in the global demand for energy and the scarcity of fossil fuels, it is necessary the development of new technologies to lessen the environmental impact and contribute to the sustainability. Therefore, renewable raw materials are an alternative for the syntheses of new monomers, polymers, solvents, and so on.[1-4]

The 2-methylenesuccinic anhydride, which is also known as itaconic anhydride (ITA) is a derivative of itaconic acid and presents elevated reactivity.[5] The main production of itaconic acid is by the fermentation of carbohydrates.[6-9] Therefore, it is considered a bio-based chemical.[5,9] Although less usual nowadays, ITA can be also obtained from the pyrolysis of citric acid.[9] ITA (Figure 1a) is a white solid, and a very reactive molecule that can be

used to obtain benzimidazoles, pyridazines, imides, and thiazoles.[10] It also provides versatile polymeric materials. Therefore, it has been extensively used to synthesize renewable copolymers, such as by reacting it with methacrylate derivatives,[11] poly(lactic acid),[12-14] hyaluronic acid,[15] chitosan derivatives,[16] starch,[17] and others.[5,18,19] The use of vegetable oils (VO) as raw materials in monomer synthesis is also interesting due to the variety of their extraction sources, such as nut, peel, and fruit seeds. In addition, some VOs are not used in the food industry and present elevated unsaturation degree (iodine value, IV) or are a waste from some industrial process; such as the grape seed oil (GSO) that presents both properties.[20] In a previous paper,[21] it was reported the evaluation of maleic anhydride (MA, Figure 1b) incorporation into soybean VO using microwave irradiation; it was verified that the most elevated incorporation into soybean VO (1.45×10^{-3} mol of MA *per* gram of soybean oil) occurred at 235 °C for 15 min. Thus, the reaction was extended to
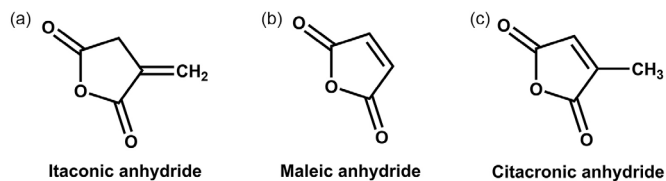
*e-mail: gilbert.bannach@unesp.br

Figure 1. Chemical structures of different anhydrides: (a) ITA, (b) MA and (c) CTA.

GSO, using same conditions, then, observing a similar amount of MA (1.79×10^{-3} mol of MA *per* gram of GSO).[20] Although both VO presented similar IV and it was used the same anhydride (MA), properties such as viscosity were significant different.

Considering the elevate reactivity and versality of modified VO by the incorporation of anhydrides into their structure, and also to produce a new monomer, it was tested the incorporation of ITA into GSO following the best condition previous described (235 °C, for 15 min, solvent-free, and using microwave irradiation). Due to the similarity between ITA and MA (Figure 1, both molecules present similar structure, and can act as enophile in the reaction), it was expected that the reaction would not present parallel reactions. However, at the end of the experiment, a black solid material was observed together with the viscous product (itaconized grape seed oil-IGSO). This was not observed in the synthesis of maleinized grape seed oil.[20] Hence, it was noted that the by-product occurred throughout the itaconization reaction, not remaining ITA.

Recently, it was demonstrated that maleic anhydride does not homopolymerize or isomerize under heating by itself under microwave irradiation and without the presence of a catalyst or solvent.[20,21] Although ITA and MA can be used in pericyclic reactions (Alder-Ene), they present different behavior under heating by microwave irradiation.

The isomerization of ITA into citraconic anhydride (CTA, Figure 1c) occurs by heating[12,13] or in the presence of a base in the synthesis of biobased polymers.[22,23] However, most studies that use ITA as a monomer do not report the effect of its isomerization into CTA or when mentioned, a deep study was not described. This phenomenon can interfere in the final properties of the material in different ways. For instance, Kučera *et al*.[12] described the decreasing of ITA solubility, as well as for the initiator, during the grafting process due to the simultaneous occurrence of ITA homopolymerization. Moreover, the final viscosity of the polymer can decrease due to undesired β-scissions chains, which were favored by increasing the amount of the initiator.[12,13] In addition, some reactions can occur less extensively due to the isomerization process, which results in a more stable

structure. For example, the Diels-Alder cycloaddition is one of the reactions used to obtain polymers based on ITA, as well as ring-opening metathesis, via radical and polycondensation.[16,18,24,25] In addition, some problems for the grafting process of poly-lactic acid (PLA) using ITA have been reported. On the other hand, the polymer resulted from the homopolymerization of ITA can act as a thermal stabilizer for common polymers, such as polystyrene and poly(methyl methacrylate); which can be considered as a positive result.[26]

Kučera *et al*.[12] studied the isomerization of ITA into CTA by heating at 90 to 190 °C and analyzed the sample by MIR (mid-infrared spectroscopy). In addition, the authors showed the homopolymerization of ITA under heating, during the radical grafting of PLA. Petrus *et al*.[13] also investigated the isomerization of ITA by heating, synthesizing a polymer from ITA in solution using azobisisobutyronitrile (AIBN) as a radical initiator. The thermogravimetric (TG) curve of ITA is shown in both papers,[12,13] however, they did not present a deep dependence of isomerization or homopolymerization on the temperatures, as well as mass losses, observed in the TG curves of ITA.

Therefore, based on the lack of literature, as well as on the previous qualitative result obtained in the utilization of ITA, as precursor in renewable monomers synthesis (it will also be further discussed) this article provides a deep characterization of ITA to investigate and well understand how its isomerization, homo or copolymerization occur by heating and by the presence of solvent (considering that these are the most commons routes for monomer and polymer synthesis). It is important to well comprehend these parameters:

(*i*) To carry out the synthesis: to avoid temperatures and solvent that can decrease the yield synthesis;

(*ii*) To provide less by-product: the CTA anhydride is more stable than ITA anhydride; then, the reaction may provide lesser products and more by-products;

(*iii*) And to clarify the structure of the products obtained: as mentioned by the literature the final properties of polymer will be affected by the possible isomerization and or/copolymerization of ITA.[5,9-11] It is possible to achieve better properties when these phenomena are well understood.

Experimental

Materials

Itaconic anhydride (ITA, 95%, Sigma-Aldrich, Cotia, Brazil), citraconic anhydride (CTA, 98%, Sigma-Aldrich, Cotia, Brazil) were used without further purifications. For high-performance liquid chromatography (HPLC) analysis, acetonitrile (HPLC grade, Sigma-Aldrich, Cotia, Brazil) and ultrapurified water were used. GSO was acquired from Mundo dos Óleos (Cruzeiro, Brazil).[27]

Characterization

Thermal analysis: thermogravimetry-differential thermal analysis (TG-DTA) and differential scanning calorimetry (DSC)

The TG-DTA curves were obtained using the equipment STA 499 F3 (Netzsch, Selb, Germany), using about 10 mg of sample and a heating rate of 10 °C min^{-1}. The analyses were performed in dry air atmosphere (70 mL min^{-1}), in the temperature range of 30-700 °C and employing an α-alumina open crucible (200 μL). The curves performed in inert atmosphere (nitrogen) were obtained in the same conditions. A DSC1 Star^e System (Mettler-Toledo, Columbus, United State of America) provided the DSC curves. Approximately 4 mg of sample was cooled to −30 °C, kept in isotherm for 3 min, and then heated to 90 °C in the first cycle. A second cycle using the same conditions was then performed. All stages were performed using a heating rate of 10 °C min^{-1} and dry air (50 mL min^{-1}).

Spectroscopic analyses: mid-infrared spectroscopy (MIR), nuclear magnetic resonance (NMR), and ultraviolet spectroscopy (UV)

The absorption spectra in the infrared region of the samples were obtained using a Vertex 70 spectrometer (Bruker, Berlin, Germany) with attenuated total reflectance (ATR) method in the region of 450-4000 cm^{-1} (32 scans at the resolution of 4 cm^{-1}) using diamond crystal. ^{1}H NMR spectra were obtained using the spectrometer Ascend III 600 MHz (Bruker, Berlin, Germany) and employing chloroform (CDCl$_3$, 99.8% D, Sigma-Aldrich, Cotia, Brazil) or dimethyl sulfoxide ((CD$_3$)$_2$SO, 99.9% D, Sigma-Aldrich, Cotia, Brazil) as solvents. UV spectra were obtained in a Cary 8854 spectrophotometer (Agilent Technologies, Santa Clara, United States of America). The analyses were run at room temperature using a quartz cuvette with an optical path of 1 cm and ethyl acetate (EtOAc, P.A. Synth, Diadema, Brazil) as solvent (1 mmol L^{-1}). Toluene (PhMe, P.A. Synth, Diadema, Brazil), acetonitrile (MeCN, P.A.

Synth, Diadema, Brazil), chloroform (CHCl$_3$, P.A. Synth, Diadema, Brazil), dimethyl sulfoxide (DMSO, ≥ 99.9% Sigma-Aldrich, Cotia, Brazil), *N,N*-dimethylformamide (DMF, ≥ 99.8% Sigma-Aldrich, Cotia, Brazil), methanol (MeOH, P.A. Synth, Diadema, Brazil), and ethanol (EtOH, P.A. Synth, Diadema, Brazil) were also used as solvents to investigate the possible solvatochromism and isomerization related to ITA.

High-performance liquid chromatography coupled to diode array detector (HPLC-DAD)

A Shimadzu LC-20AT System (Shimadzu, Koriyama, Japan) equipped with an SPD-M20 DAD detector was employed. The equipment has an autosampler model SIL-20A HT and a CTO-10AS column oven. A Phenomenex Luna(2) C$_{18}$ column (250 × 4.6 mm, 5 μm), and a guard column were used. The LC solution software was used for controlling the analytical system and for data analysis. For the analysis, water:acetonitrile mobile phase in the ratio of 95/5 (v/v), were passed through HPLC system for 1 h at 1 mL min^{-1} flow rate. The total injection volume was set to 5 μL. All samples were prepared using 10 mmol L^{-1} and those identified as heated in the Results and Discussion section (UV and HPLC-DAD analysis) were prepared by ITA heating until the specific temperature. For instance, the sample heated until 150 °C was named as ITA-150. The HPLC-DAD chromatograms were monitored at 220 nm (related to ITA) and 240 nm (related to CTA).

Analysis of renewable monomers and the respective precipitates obtained after the incorporation of itaconic anhydride into grape seed oil by microwave irradiation

The incorporation process of ITA into GSO (itaconization) was performed following the procedure described in a previous paper,[20] at three different temperatures: 120, 180, and 235 °C. The respective precipitate was separated from the itaconized grape seed oil by centrifugation, then washed with ethyl acetate and dried at 60 °C for 10 min. Samples were named as P followed by the reaction temperature (P120, P180 and P235). They were analyzed by TG-DTA (using the same conditions aforementioned) and by UV-Vis (in CHCl$_3$ due to the sample mutual solubility and to avoid parallel reactions). The monomers (itaconized grape seed oil) were named as IGSO followed by the temperature in which it was obtained. For instance, IGSO-120 was obtained at 120 °C. To determinate the amount of anhydride incorporated into GSO an acid-base potentiometric titration was executed. So, 0.4 g of sample was solubilized in acetone (30 mL) and 1 mL of distilled water was added into the system. Thus, the system was closed and heated up to 60 °C and kept in this

temperature for 30 min. Thereafter, the system cooled down to room temperature and the sample was titrated against a NaOH aqueous solution (0.1 mol L^{-1}) previous standardized with potassium hydrogen phthalate. The titration was performed in triplicate and in all experiments an automatic burette was used (model Digitrate Pro 50 mL, Jencons).

Results and Discussion

As aforementioned, the ITA was incorporated into GSO by a microwave irradiation heating without solvent or catalyst to provide the renewable monomer (itaconized grape seed oil- IGSO). The synthesis was performed at three different temperatures (120, 180 and 235 °C) for 15 min.[20] As observed in Figure 2a, at the end of experiment and after the system centrifugation for separation of residual anhydride, it was observed a black solid in the bottom of each flask (magnified also in Figure 2a).

The decreasing temperature of synthesis to 180 and to 120 °C also provided a solid by-product (Figures 2b and 2c). Their color and solubility varied among the synthesis. Thus, to better evaluate what occurred with ITA during the synthesis, it was performed several studies. The first one was the evaluation of its thermal behavior.

Thermal behavior of ITA

For thermal behavior of ITA it was expected a melting process followed by complete sample evaporation, as observed for maleic and succinic anhydrides.[28] However, the thermal profile of ITA (Figure 3a) was different. Under air atmosphere, it melted ($T_{melt\ Air}$) at 72 °C, as evidenced by the endothermic peak in DTA curve without mass loss.
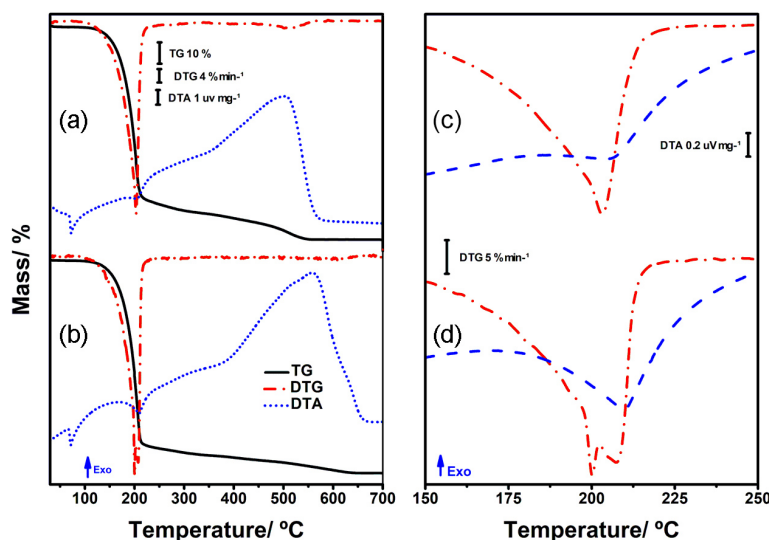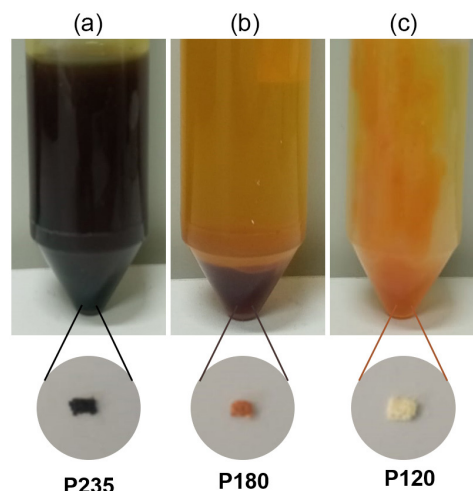

Figure 2. Reaction mediums obtained after itaconic anhydride incorporation into grape seed oil by microwave irradiation in different temperatures, as well as the precipitated obtained in each synthesis: (a) 235 °C, (b) 180 °C, and (c) 120 °C.

In addition, at 105 °C it was observed the beginning of the first mass loss (105-217 °C, $\Delta m = 79.69\%$) which resulted in an endothermic peak in DTA curve ($T_p = 204$ °C) that was associated to the evaporation of ITA. This event resulted in a maximum evaporation rate (MER) of 28.8% min^{-1}, and the temperature of maximum evaporation rate (T_{MER}) was 203 °C. However, this endothermic event was less intense than endothermic events usually observed for the evaporation process of small anhydrides, such as maleic and succinic anhydrides.[28] This associated with the consecutive and continuous mass loss, observed from 217 to 561 °C ($\Delta m = 19.79\%$) in TG/DTG curves, suggested that the presence of a double bonding between the methylene group, and the five-membered anhydride structure (Figure 1a) strongly interfere in ITA decomposition.

Figure 3. TG/DTG-DTA curves of ITA (itaconic anhydride) in (a) dry air atmosphere, (b) N$_2$ atmosphere as well as magnification between 150 and 250 °C under (c) air atmosphere, and (d) N$_2$ atmosphere.

For better evaluation, the thermal profile of ITA was evaluated under inert atmosphere (N_2), and the resulting curve can be seen in Figure 3b. As expected, the melting process was not affected by the atmosphere ($T_{melt\ N2}$ = 72 °C). ITA under N_2 was stable up to 104 °C, and the first mass loss finished at 217 °C; both values are similar to those observed under air atmosphere (Figure 3a). Although the TG curves profiles in air and N_2 were very similar, the mass loss (Δm) of this step was higher in N_2 than observed in air (Δm_{N2} = 85.48%, Δm_{air} = 79.69%). As a consequence, the endothermic peak ($T_{p\ N2}$ = 210 °C) for this event was more intense and sharper than observed in air atmosphere (Figure 3a). In addition, instead of one, two consecutive peaks were observed in the DTG curve (Figures 3c and 3d, respectively). One at T_{MER} = 200 °C (MER = 32.7% min^{-1}) and another related to maximum degradation rate (temperature of maximum degradation rate (T_{MDR}) = 207 °C; maximum degradation rate (MDR) = 31% min^{-1}). This change in DTG curve suggested that the phenomenon responsible for the mass loss changed, resulting in a broad and continuous mass loss (second one) in TG curve. Beside this step occurred at a higher temperature range (217- 644 °C) than in air (217-561 °C), its resulting exothermic peak in DTA was also displaced to

higher temperatures (T_p = 558 °C) and was also more intense than that in air atmosphere (T_p = 501 °C). Although the difference between the temperature range and an exothermic event in DTA curve, the phenomenon under air or nitrogen atmosphere appeared to be the same type of decomposition (radical decomposition), which will be further clarified.

Determination of products obtained from ITA heating

To clarify its thermal profile, ITA was heated based on the TG curve to different temperatures (130, 150, 175, 200, 210, 250, and 300 °C). For each temperature, it was analyzed the non-volatile material, as well as the volatile material, which was condensed on a glass slide and analyzed by MIR (Figure 4). In addition, the video recording of ITA heated from 30 to 300 °C (10 °C min^{-1}) is available as Video S1 (Supplementary Information section). The blue arrows in Figure 4 indicate the main bands in ITA spectrum, which were centered at 1762 cm^{-1} (C=O stretching), 1668 cm^{-1} (C=C stretching), and 929 cm^{-1} (CH$_2$=C out-of-plane deformation) and are in agreement with those reported by Kučera *et al.*[12] The carbonyl band of CTA (Figure 4) appeared at 1755 cm^{-1}, while the bands at 1649 and 865 cm^{-1} referred to C=C stretching and C=CH of
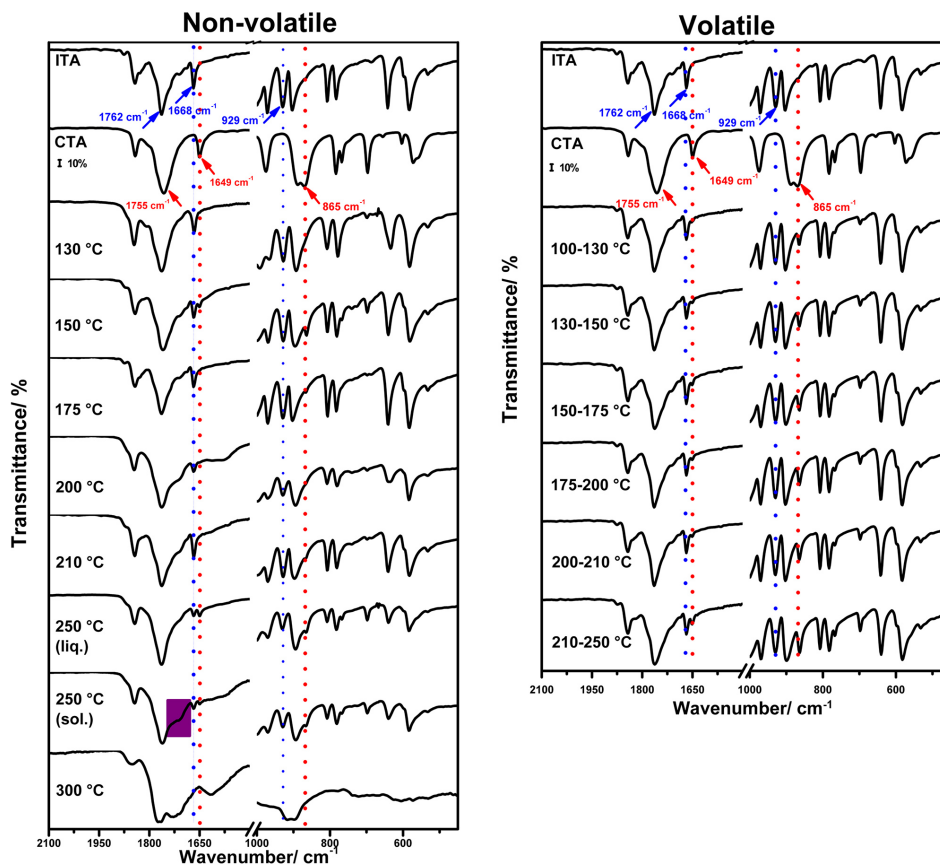

Figure 4. MIR spectra of ITA (itaconic anhydride) heated until different temperatures.

CTA (pointed by red arrows), respectively. Video S1 shows that close to 100 °C part of the sample started to evaporate. However, up to 130 °C, a visual change was not observed in the spectrum of non-volatile material (Figure 4). The volatile material exhibited all bands associated with ITA and others at 865 and 1649 cm^{-1}, which are associated with the CTA. At 150 °C it was noticed in the spectrum of non-volatile sample, that the intensity of the band associated with C=C stretching of ITA (1668 cm^{-1}), decreased; while the band associated with the same stretching for CTA exhibited similar intensity.

At 175, 200 and 210 °C, the bands at 1650 and 864 cm^{-1} (CTA) almost vanished in non-volatile sample, while in spectra of the volatile sample, they remained up to 250 °C. These results indicated that CTA started to form in the system followed by an evaporating process (the system was liquid and yellowish as can be seen in Video S1).

Moreover, both bands attributed to CTA increased at higher temperatures, indicating ITA was converted into CTA, which was evaporated from the system. By TG/DTG-DTA curves (Figure 3a) it was evidenced that the first mass loss and the endothermic event ended at 222 °C (sample was completely yellow, Video S1). As aforementioned, at this temperature the rate of mass loss decreased, suggesting that the ITA and CTA evaporation was not the major phenomenon, but still occurred, as observed in the spectrum of the condensed sample at 250 °C (Figure 4). At this temperature, the remaining sample (non-volatile) exhibited an orange-reddish color (Video S1). However, a mixture between liquid and solid states was noted. The phases were separated, and the resulting spectra can be seen in Figure 4 (250 °C liq. and 250 °C sol.). Although their similarity, the large shoulder between 1728 and 1702 cm^{-1} in the spectrum of the solid sample suggests

that, a new carbonyl band overlapped those of ITA and CTA (highlighted in purple in Figure 4); indicating a possible polymerization (a new carbonyl from the polymer).

To evaluate the ITA isomerization and polymerization processes under heating, ITA was heated in TG and analyzed by ^{1}H NMR (Figure 5). The ^{1}H NMR spectrum of ITA without heating (Figure 5a) exhibited three signals: two triplets with a chemical shift at 6.58 (J_3 5.2 Hz, J_2 2.7 Hz) and 5.93 (J_3 4.8 Hz, J_2 2.7 Hz) ppm, related to the vinylic hydrogens Ha and Ha', respectively. Furthermore, the spectrum showed another triplet at 3.63 ppm (J_3 5.8 Hz, J_3 2.7 Hz), which refers to the cyclic hydrogens Hb. After heating ITA up to 230 °C (Figure 5b), new signals were observed. In addition to the triplets from ITA structure (Ha, Ha', and Hb), the singlet at 6.58 ppm, assigned to the hydrogen Hc and the singlet at 2.21 ppm from the methyl hydrogens Hd were observed, which confirmed the isomerization of ITA into CTA when heated. The polymer structure derived from ITA and CTA can also be observed in the spectrum (Figure 5b). This was confirmed by the signals between 3.27-3.22 ppm (He, q, J 18.64 Hz), 3.05-3.02 ppm (He', q, J 14.97 Hz), and 2.89-2.83 ppm (Hg, sxt, J 18.65 and 14.97 Hz) and at 2.16 ppm (Hf, s). Therefore, it suggested that at 230 °C, the anhydrides began to be copolymerized by a radical process.

As observed in TG/DTG-DTA curves (Figure 3) and supported by Video S1, the radical decomposition, of ITA occurred after 270 °C. The thermal degradation was confirmed by the changes in MIR spectrum (Figure 4, 300 °C), in which most bands are deformed.

The TG/DTG-DTA curves (performed in dry air atmosphere at same conditions described in the Experimental section) of CTA and ITA sample heated to 250 °C are shown in Figure S1 (in Supplementary Information (SI)
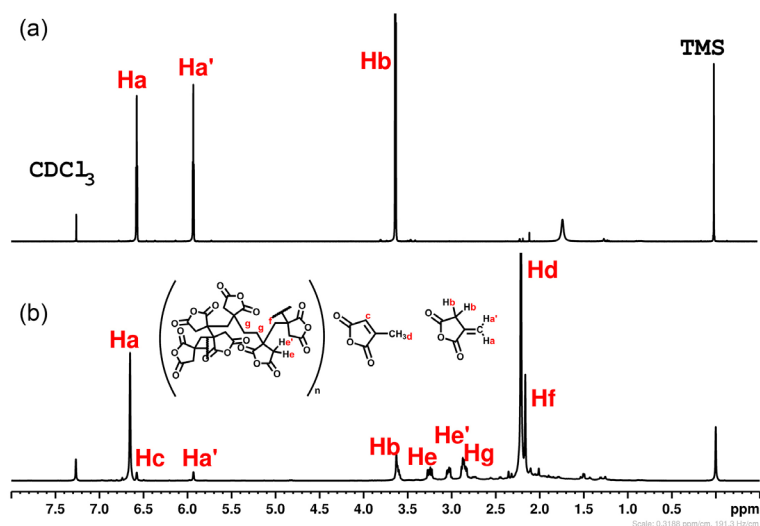

Figure 5. ^{1}H NMR spectra (600 MHz, CDCl$_3$) of ITA (itaconic anhydride) at (a) 25 °C and (b) heated to 230 °C in TG-DTA system.

section) along with the related discussion. They suggest the presence of ITA and CTA in the sample heated until 250 °C as well as indicate the presence of a by-product (different from the previous anhydrides), which may be the polymer resulted from the homo or copolymerization of anhydrides. The main indicative is the increasing of the value of the second mass loss ($\Delta m = 30.37\%$), indicating a more crosslinked material. However, this will be better discussed in the following sections.

UV and HPLC-DAD analysis

To corroborate the previous results, HPLC-DAD analysis was performed. Although the isomerization of ITA into CTA in solution was previously cited,[13] in the present paper the solvent dependence of ITA in different organic solvents was evaluated (Figure 6a) aiming to support these results and also to select the appropriate solvent to be used in the HPLC-DAD analysis. The resulting UV spectra are shown in Figure 6b.

ITA is soluble in several organic solvents such as ethanol, DMSO, DMF, ethyl acetate (EtOAc), toluene, methanol (MeOH), and acetonitrile (MeCN). A linear correlation was not observed between the maximum absorptions in UV spectra and the polarities of the solvents. In addition, the maximum absorptions bands observed in each spectrum indicated that some polar solvents showed

lower absorption than nonpolar solvents. Then, the results suggested that a less polar excited state than the initial state (ground state) will be better established in less polar or non-polar solvents, requiring higher energy for excitement, and leading to a hypsochromic shift of the maximum absorption (negative solvatochromism).[29-32] This explains the behavior of ITA in the polar solvents EtOH ($\lambda_{max} = 221$ nm), MeCN ($\lambda_{max} = 222$ nm), and EtOAc ($\lambda_{max} = 254$ nm). Moreover, EtOH is a polar protic solvent, with the ability to act as a hydrogen bond donor, which can induce the formation of stable solute-solvent interactions in the ground or excited electronic states, resulting in changes in the absorption shift.[30,32,33]

Otherwise, ITA in the non-polar solvents PhMe ($\lambda_{max} = 284$ nm) and CHCl$_3$ ($\lambda_{max} = 243$ nm), exhibited an unexpected dependence since higher values of wavelength absorptions (compared to the polar solvents) were expected. Moreover, CHCl$_3$ has the ability of a weak hydrogen donor, generating a solute-solvent interaction, and resulting in a hypsochromic effect compared to PhMe.[30,32,33] The solvents DMF ($\lambda_{max} = 266$ nm) and DMSO ($\lambda_{max} = 264$ nm) provided a significant bathochromic shift in the spectra. Both solvents are considered as a basic Lewis donor, in which DMF can act as a soft solvent due to nitrogen donor atom; whereas, DMSO can act as a soft/hard solvent due to its soft sulfur donor atom and the hard oxygen donor atom, respectively.[30,32,34] This can result in solute-solvent
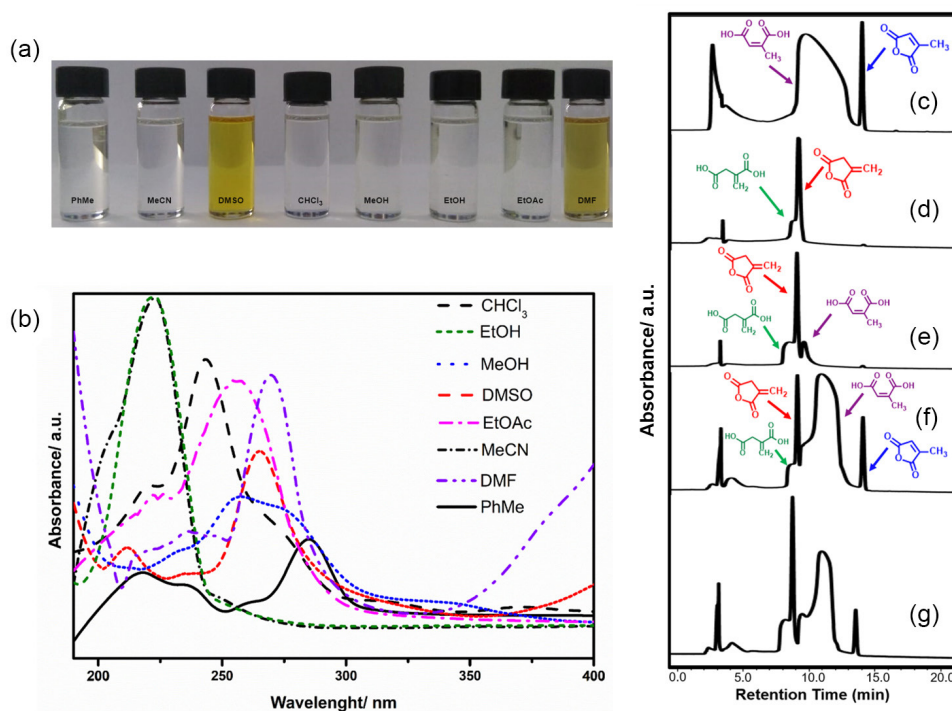

Figure 6. (a) ITA (itaconic anhydride) solubilized in different organic solvents, (b) UV spectra of ITA in different organic solvents (1 mmol L^{-1}), and HPLC-DAD chromatograms obtained for samples, (c) CTA (citraconic anhydride), (d) ITA, (e) ITA heated to 150 °C, and ITA heated to 250 °C, (f) non-volatile sample and (g) volatile sample.

interactions in solution, establishing the excited state, and generating bathochromic shifts. Although most solutions were coreless (Figure 6a), the solutions of DMSO and DMF are yellow. This change in their color was observed immediately after ITA solubilization, suggesting some different interaction with these solvents.

Some authors have reported the ITA isomerization into CTA during polymerization reactions that demanded heating in the DMSO presence. To clarify if DMSO can undergo this isomerization, it was performed a ¹H NMR analysis of ITA in $(CD_3)_2SO$ and the resulting spectrum can be seen in Figure S2 (SI section). It supported the isomerization into CTA in DMSO medium. Moreover, the presence of water in the solvent allowed the formation of citraconic acid (methylmaleic acid). The signals from ITA were observed between 6.30-6.28 ppm (Ha, 1H, t), 5.90-5.89 ppm (Ha', 1H, t), and 3.66-3.64 ppm (Hb, 2H, t), while the signals from CTA were in the range of 7.09-7.08 ppm (Hc, 1H, dd) and 2.08-2.07 ppm (Hd, 3H, d). Finally, the hydrogens from citraconic acid presented a chemical shift at 13.02 ppm (COOH, He/He', 2H, s) and 2.07 ppm (Hf, 3H, s), and the signal of Hc overlapped with the Hc signal in the double doublet at 7.09-7.08 ppm.[35,36] These results explained the yellow color of ITA in DMSO (Figure 6a), which can be assigned to the formation of other compounds (the same observed in the deuterated solvent in NMR analysis).

A suggestion of the reaction mechanism is exhibited in Figure S3 (SI section). The oxygen from the DMSO molecule was responsible for withdrawn an allylic hydrogen from ITA structure, allowing the isomerization to CTA. Then, the oxygen from the sulfoxide group does a nucleophilic attack to the carbonylic carbon of the CTA, opening the ring and generating an intermediary sulfur ionic complex. The water content present in the solvent was responsible for stabilizing the intermediary, forming the citraconic acid.

Based on UV spectra of ITA and its ¹H NMR in $(CD_3)_2SO$, it was performed a HPLC analysis to better investigate ITA behavior in solution. The resulting chromatograms are in Figures 6c to 6g. The first chromatogram (Figure 6c) was related to the CTA, and displayed two chromatographic bands with retention time at 10 min and approximately 15 min. The first band was associated with citraconic acid as confirmed by the UV_{max} at 220 nm. The CTA can be easily hydrolyzed in the presence of water (the eluent solvent was $MeCN/H_2O$); thus, the second band was associated with the CTA with UV_{max} at 210 nm and a shoulder at 239 nm, which was consistent with findings in UV study. The chromatogram for ITA (Figure 6d) exhibited an overlapped chromatographic band at 9 min related to ITA and itaconic

acid with a UV_{max} at 213 nm, which was in accordance with UV results. Furthermore, the chromatographic band at approximately 15 min could be associated with CTA. The third chromatogram (Figure 6e) was related to ITA-150, which was similar to the second chromatogram, except for a band at 10 min that could be related to citraconic acid. The chromatogram for sample ITA-250 (Figure 6f) was very similar to ITA-150 (Figure 6e); however, the chromatographic bands related to citraconic acid (10 min) and CTA (15 min) were greater, which confirmed the isomerization process by heating (ITA CTA). The last chromatogram referred to volatile sample collected from ITA-250 (Figure 6g) and exhibited all bands described for the non-volatile sample, confirming the presence of ITA and CTA at this temperature.

DSC analysis

Figure 7 exhibits the DSC curves obtained for different samples. The ITA (Figure 7a) exhibited 99.7% purity, and as expected, thermal events were not observed in the first cooling. In the first heating, an endothermic peak at 70.7 °C was observed and it referred to its melting. In the second cooling, it crystallized at 6.7 °C, as evidenced by the exothermic peak. In the second heating, the melting process was repeated without modifications (Figure 7a, Table 1). CTA is a liquid anhydride, and under the experimental conditions performed, it did not crystalize, as observed in Figure 7b and Table 1.

The other DSC curves (Figures 7c to 7f) were obtained immediately after heating ITA to different temperatures (non-volatile samples). The sample heated to 150 °C (Figure 7c) exhibited similar behavior as ITA; however, a small decrease of melting temperature (T_{melt}) and associated enthalpy (ΔH_{melt}) occurred (Table 1). This was expected considering that at this temperature, part of ITA was converted into CTA, which acted as an impurity, decreasing the sample purity to 98.3%. As observed in Table 1, with the decreased of purity, the melting and crystallization temperatures increased, corroborating with the increase of CTA in the system.

Heating ITA to 250 °C provided a sample part in the liquid state and the solid state. As a result, it was obtained two samples at this temperature, and they were named as 250 liq. (the liquid one) and 250 pol. (the solid one) in Figure 7 and Table 1. The sample 250 liq. (Figure 7e) exhibited a melting process in the first heating at 58.2 °C and ΔH_{melt} = 10.8 kJ mol⁻¹. However, the sample crystallized at −23.6 °C at the end of the second cooling. As a result, part of the sample could be amorphous,[37,38] resulting in a glass transition at −5.2 °C in the second heating (pointed
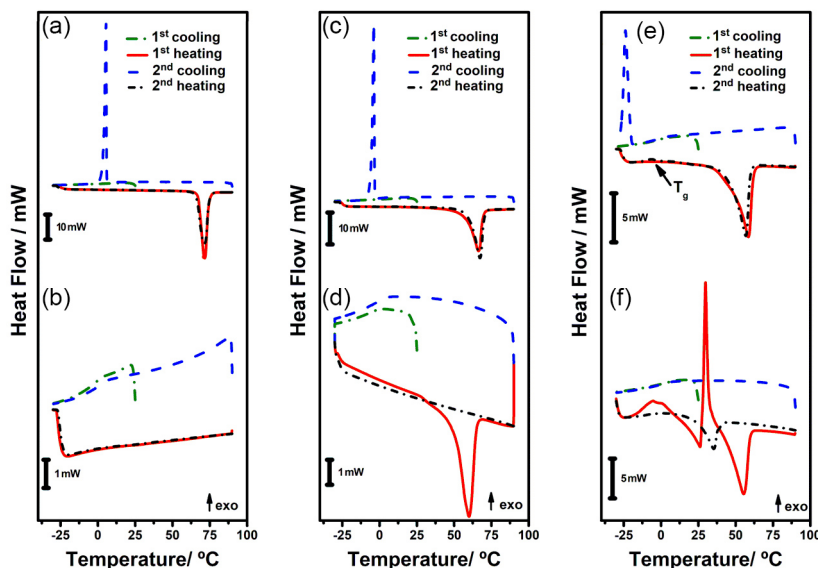
Figure 7. DSC curves of (a) ITA (itaconic anhydride), (b) CTA (citraconic anhydride), (c) ITA heated to 150 °C, (d) ITA heated to 210 °C, and ITA heated to 250 °C, (e) liquid sample and (f) solid sample (copolymer).

Table 1. Values of purity (calculated by Van't Hoff equation), temperature of glass transition ($T_{g\ midpoint}$), temperatures of crystallization (T_{cryst}), and melting (T_{melt}) as well as enthalpies of crystallization (ΔH_{cryst}) and melting (ΔH_{melt}) obtained by the DSC curves for itaconic anhydride (ITA), citraconic anhydride (CTA), and ITA previous heated until different temperatures[a]

Sample	Purity / %	$T_{g\ midpoint}$ / °C	T_{cryst} / °C	ΔH_{cryst} / (kJ mol^{-1})	T_{melt} / °C	ΔH_{melt} / (kJ mol^{-1})
ITA	99.7		—[b] 6.7[d]	—[b] 11.6[d]	70.7[c] 70.5[e]	14.6[c] 14.3[e]
CTA	—	—	—	—	—	—
150[a]	98.3	—	—[b] −2.5[d]	10.4[c]	66.5[c] 66.7[e]	11.0[c] 11.9[e]
210[a]	97.6	—	—	—	59.8[c]	5.9[c]
250 liq.[a]	92.9	−5.2[d]	—[a] −23.6[d]	—[a] 5.4[d]	58.2[c] 56.5[e]	10.8[c] 8.8[e]
250 pol.[a]		−2.7[b]	—[a] 30.3[c]	—[a] 4.8[c]	55.0[c] 21.7[e]	5.9[c] 2.4[e]

[a]Samples obtained by heating the ITA up to these temperatures (°C). For instance, sample 150 means that ITA was previously heated until 150 °C and then, a DSC curve was performed; [b]1st cooling; [c]1st heating; [d]2nd cooling; [e]2nd heating; ITA: itaconic anhydride; CTA: citraconic anhydride.

by an arrow in Figure 7e), which corroborated with the decreasing of ΔH_{melt} from 10.8 kJ mol^{-1} (observed in the first heating) to 8.8 kJ mol^{-1} in the second heating. The DSC curve obtained for the copolymer resulting from radical polymerization between ITA and CTA is shown in Figure 7f. Although no event was observed in the first cooling or on the surface of the sample (Figures 8a and 8b), a glass transition and a cold crystallization (exothermic peak) occurred in the first heating at −2.7 °C and 30.3 °C (Table 1), changing the surface of the sample (Figures 8c to 8f). These events occurred due to a fast-cooling process after heating ITA to 250 °C before the DSC analysis, and they are more visible in Figure 8 and Video S2. In addition, part of the sample melted (Figures 8g and 8h), resulting in an endothermic peak at 55.0 °C in DSC curve (Figure 8f). The melting process can be associated with residual ITA

and CTA that were present inside of the polymer chain (cage effect), corroborating the results obtained by TG/DTG-DTA, MIR, and HPLC.

Performing a controlled cooling (10 °C min^{-1}) and when the sample was maintained at −30 °C (3 min), no thermal events were observed in the DSC curve (Figure 8f) or on the surface of the sample (Figures 8j and 8k). Therefore, only the endothermic peak in the second heating was observed and referred to the melting of the residual anhydrides (Figures 8m and 8n). As can be seen in Video S2 and in Figure 8, the copolymer obtained with the heating of ITA up to 250 °C did not melt when heated, which agrees with the thermal behavior observed in its TG/DTG-DTA curve (Figure 5b).

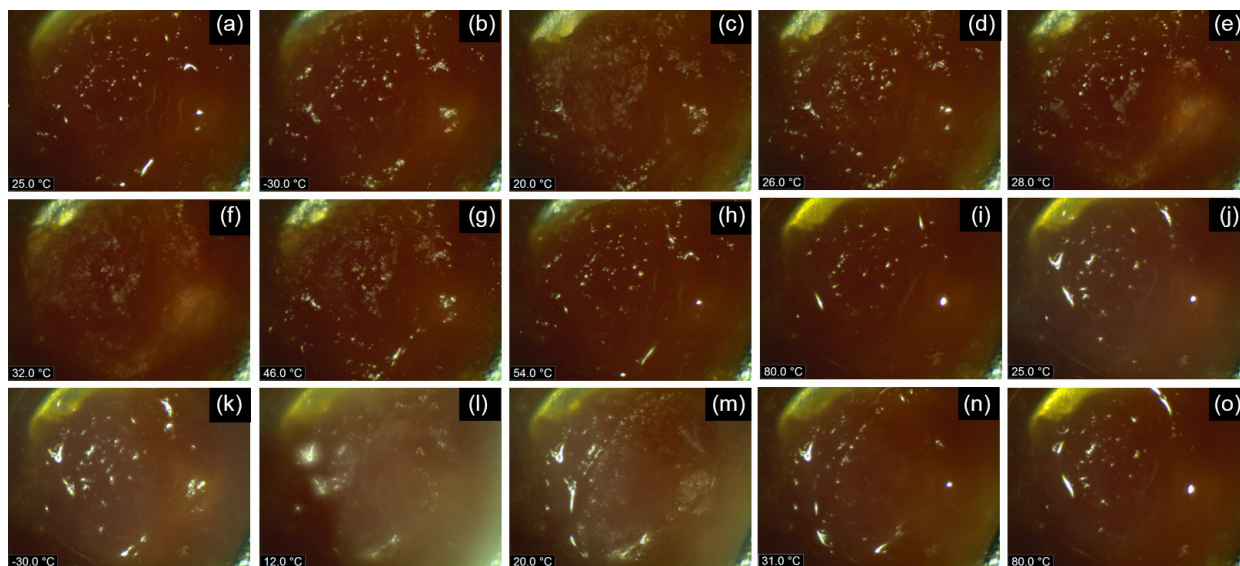All previous results suggest that ITA begins the conversion to CTA near 100 °C; however, all CTA

Figure 8. Images obtained from copolymer (by radical polymerization) from ITA (itaconic anhydride) and CTA (citraconic anhydride) by heating and then submitted to different DSC stages: First cooling (a and b); first heating (c to i); second cooling (j and k); second heating (l to o).

evaporated from the system by 150 °C, the temperature which was also found for the non-volatile product. Therefore, most of the first step of mass loss in TG curve referred to the ITA and CTA evaporation. However, the end of this mass loss indicated the formation of a copolymer followed by the decomposition of the sample, which continued in the second step of mass loss and was strongly affected by the atmosphere type. The end of the first mass loss and the second one could be attributed to a radical process. Therefore, in air atmosphere, this phenomenon could be favored by the presence of molecular oxygen, which is in the triplet state and thus can initiate the radical process. Under an inert atmosphere, this process also occurred; however, the evaporation process was more favored than the copolymerization process, as evidenced by the more intense peak in DTA curve and higher value of mass loss (Figure 3b). Moreover, at around 270 °C the sample began to decompose, as observed by the color change from orangish-red to brownish red in Video S1, and by the changes in MIR spectrum at 300 °C (Figure 4). The decomposition process was also a radical process, which can be extended from the copolymerization. This was corroborated by the absence of carbonaceous residue at 700 °C under inert atmosphere (Figure 4b) and by the similarity of the profile of the DTA curves (resulting from the second step of mass loss) obtained in air and nitrogen atmospheres. Therefore, based on TG/DTG-DTA, MIR, and NMR results it is suggested the following thermal decomposition of ITA (Figure 9).

Based on the previous results, it was possible to clarify the precipitate observed in the reaction mediums obtained after the itaconic anhydride incorporation into GSO at different temperatures (Figure 2). The TG/DTA-DTA curves, as well as the respective mass loss and temperature ranges, obtained for each precipitate, can be seen in Figure S4 and Table S1 (SI section). For P120, it was observed a small mass loss (3.69%) between 30 and 133 °C, which can be associated with the presence of CTA in the precipitate from the synthesis. This mass was higher for the sample P180, which was expected due to the increase of temperature, resulting in a sample with a dark orange color (Figure 2b). As aforementioned, the polymerization process started at 230 °C, and at 270 °C the radical decomposition process was observed. However, as observed and evidenced by TG-DTA/DTA curves, an isothermal process at 235 °C is enough to polymerize almost all non-incorporated anhydrides (resulting in a small mass loss between 30 and 230 °C), and also to begin the radical decomposition process.

Figure S5 (SI section) exhibits the UV-Vis spectra of precipitates, ITA (UV_{max} = 243 nm) and CTA (UV_{max} = 250 nm). It was noticed that P120 and P180 presented the bands associated with both anhydrides ITA and CTA, while P235 showed the band associated to ITA. A new large band (between 280 and 330 nm) was observed in the spectra of P180 and P235, suggesting the presence of the copolymer in these precipitates. The MIR spectra of precipitates (Figure S6, SI section) corroborate these results: the band associated to $H_2C=C$ out-of-plane deformation of ITA (929 cm^{-1}) appeared in all precipitate spectra. Whereas, the band associated to C=CH of CTA (865 cm^{-1}) was observed in P120 and P180 spectra. These results suggest that CTA obtained by the ITA isomerization was almost completely consumed in the copolymerization process during the itaconization reaction. Therefore, unlike
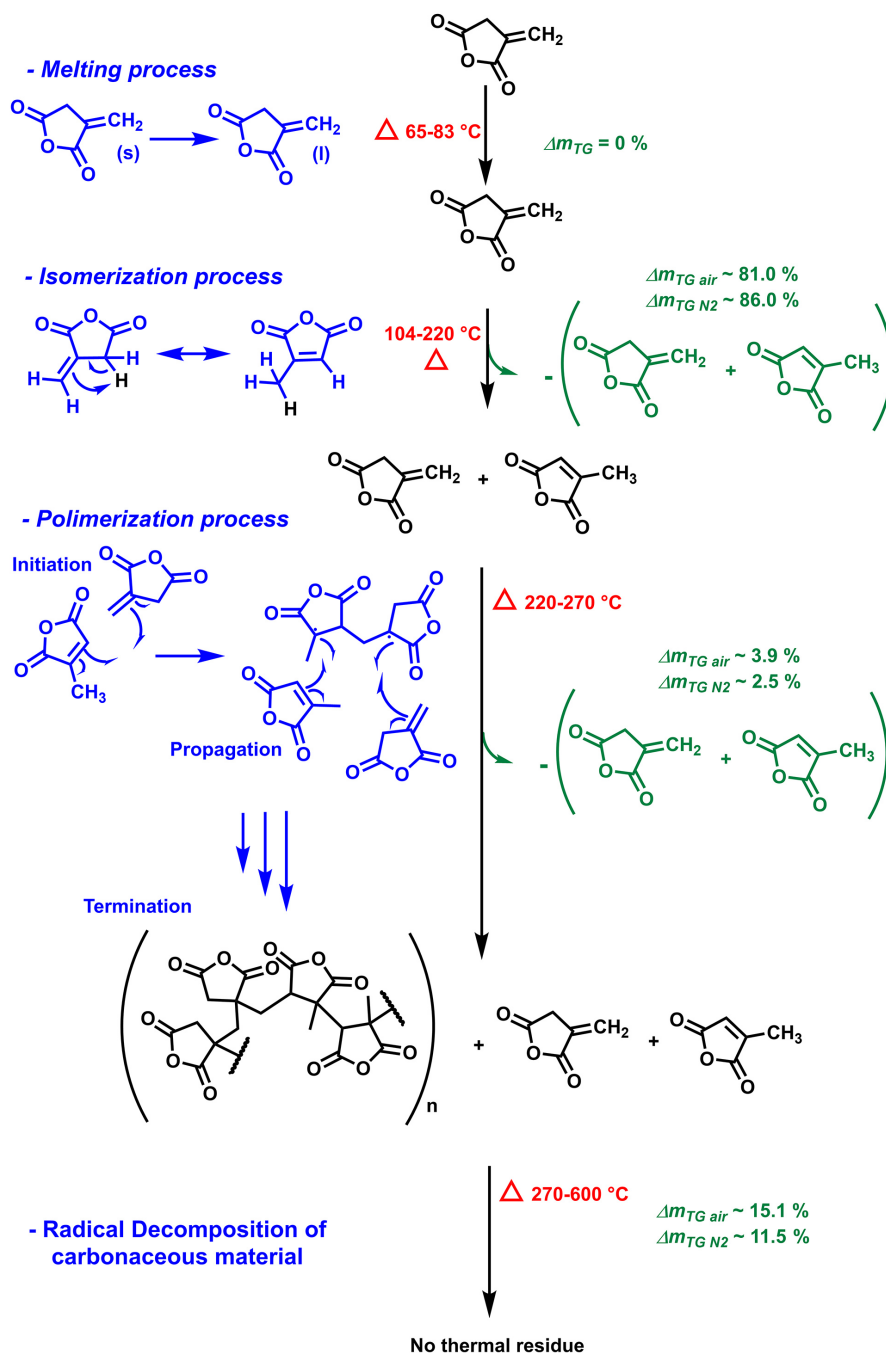
Figure 9. Thermal processes associated with ITA (itaconic anhydride) submitted to heating under air and inert (N_2) atmosphere (suggested mechanism).

performed for maleic anhydride, it is not possible to recover and reuse the residual anhydride after the incorporation process into vegetable oils.

The results of acid-base titration of IGSO samples (the interest monomers) are present in Table 2, and they indicated that the incorporation of anhydride into GSO at 120, 180, and 235 °C increased proportionally with the temperature. This tendency was expected, since the incorporation of maleic anhydride into soybean oil also increased when the experimental conditions were evaluated.[21] However, as

aforementioned, it was expected that the incorporation of ITA into GSO structure (at 235 °C for 15 min) would be similar to that obtained with MA and it was near to 18% lesser.[21] This decreasing of anhydride incorporation amount can be related to the difference of reactivity between the enophiles MA (a double α,β-unsaturated carbonyl compound) and ITA (an α,β-unsaturated carbonyl and a β,γ-unsaturated carbonyl compound). Another point is resulted from the parallel reactions of ITA isomerization and then the polymerization of ITA and CTA.

Table 2. Amount of anhydride incorporated *per* gram of sample temperature ranges (θ), experimental mass losses (Δm), maximum degradation rate (MDR), temperature of maximum degradation rates (T_{MDR}), and temperature of peak (T_p) observed for each step of mass loss in TG/DTG-DTA curves of GSO (grape seed oil) and IGSO (itaconized grape seed oil) samples

Step of mass loss		GSO	IGSO-120	IGSO-180	IGSO-235
	Amount of anhydride[a] / (mols of anhydride *per* g of sample)	–	$(1.7 \pm 0.1) \times 10^{-4}$	$(3.9 \pm 0.3) \times 10^{-4}$	$(14.6 \pm 1.0) \times 10^{-4}$
1st	Δm / %	50.31	45.48	36.66	34.13
	θ / °C	270-394	268-392	250-381	217-370
	T_p / °C	361 ↑	369 ↑	363 ↑	360 ↑
	T_{MDR} / °C MDR / (% min⁻¹)	357/7.1	366/7.6	357/6.3	351/5.0
2nd	Δm / %	32.40	36.84	46.79	46.51
	θ / °C	394-472	392-465	381-475	370-466
	T_p / °C	423 ↑	420 ↑	398 ↑ 421 ↑	421 ↑ 438 ↑
	T_{MDR}/ °C MDR / (% min⁻¹)	415/13.5	417/10.6	394/6.1 418/11.1	419/8.6
3rd	Δm / %	15.15	15.78	14.12	16.60
	θ / °C	472-599	465-601	475-603	465-599
	T_p / °C	502 ↑	496 ↑	501 ↑	497 ↑
	T_{MDR}/ °C MDR / (% min⁻¹)	528/2.1	536 / 2.0	534/1.9	530/2.2

[a]Calculated by acid-base titration; IGSO-120 (itaconized grape seed oil obtained at 120 ℃), IGSO-180 (itaconized grape seed oil obtained at 180 ℃), and IGSO-235 (itaconized grape seed oil obtained at 235 ℃); ↑ exothermic peak.

Figure 10a exhibits the MIR spectra for GSO and all IGSO samples. The IGSO-120 spectrum was very similar to GSO, while in IGSO-180 spectrum the bands resulted from anhydride incorporation (1857, 1782, and 1708 cm⁻¹) are more visible; however, as expected due to the higher amount of anhydride, they are more evident in the IGSO-235 spectrum. Beside this region (highlighted in purple in Figure 10a), any other modification was observed in MIR spectra (due to the similarity between IGSO and GSO structure). Moreover, due to their similarity is not

possible attribute bands for ITA or CTA since considering that the incorporation of both anhydrides would result in the consumption of their double bonds.[20,21] Thus, using MIR is possible to identify the incorporation anhydride without attribute with one was incorporated.

The TG/DTG-DTA curves of GSO, and the IGSO samples are shown in Figure 10b, while the steps of mass loss, temperature ranges, and events in DTA curves are shown in Table 2. It is observed that after the anhydride incorporation, all samples had their thermal stability
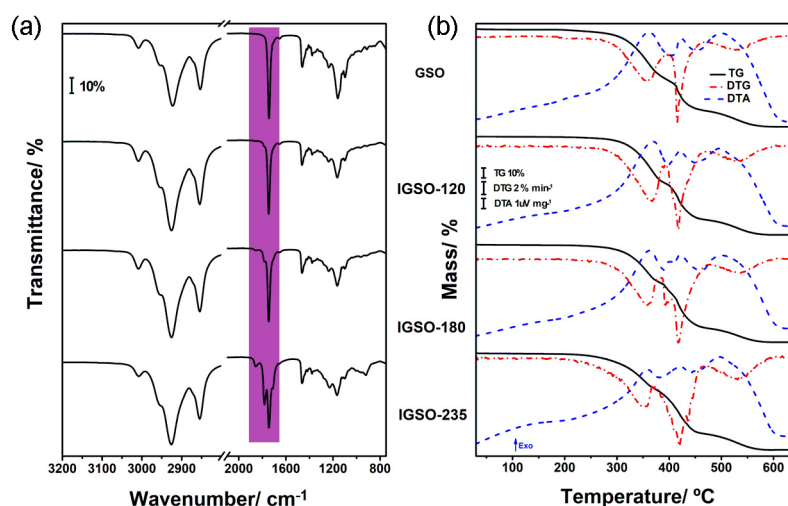

Figure 10. (a) MIR-ATR spectra and (b) TG/DTG-DTA curves obtained for GSO (grape seed oil) and the IGSO (itaconized grape seed oil) samples obtained at different temperatures: 120 °C (IGSO-120), 180 °C (IGSO-180), and 235 °C (IGSO-235) under microwave irradiation.

decreased compared to GSO (270 °C), and as the amount of anhydride increases, the thermal stability decreased (IGSO-120 < IGSO-180 < IGSO-235). In addition, it is seen by the DTG curves (magnified in Figure S7) that as the anhydride amount increases in the structure the T_{MDR}, as well as the MDR, decreased in the first mass loss (Table 2). Then, indicating more resistance of chain in thermal degradation. This tendency of decreasing of the MDR values is also observed for the second mass loss (Table 2 and Figure S7, SI section). However, the third mass loss was not considerable affected by the anhydride incorporation. These results may be attributed to in IGSO samples, the decomposition started by the side chains in monomers, which increased with the anhydride amount. As a result, the first and second mass losses are affected, since these steps are mostly resulted from the mono e polyunsaturated chains in GSO. Therefore, they will be affected by the anhydride incorporation. On the other hand, the last step of mass loss in TG curve of GSO are mainly resulted from the saturated chains, consequently they are not modified by anhydrides incorporation, which justifies the non-significant change of this step in GSO compared to all IGSO samples.

Conclusions

According to TG/DTG-DTA results, the ITA melted at 72 °C and immediately began to evaporate. However, in evaporate sample (volatile one), the CTA was also found, which resulted from the ITA isomerization. The isomerization process increased with temperature, resulting in a yellowish liquid sample. Both anhydrides submitted to heating resulted in the beginning of the copolymerization (orange-reddish material) process at 230 °C, as indicated by the MIR and ^{1}H NMR results. Finally, based on the combination of all techniques, a mechanism was proposed to demonstrate how ITA behaved under heating and how the CTA formation. These results (associated with the titration, MIR and TG/DTG-DTA of IGSO in different temperatures) suggest that performing the reaction under low temperatures is not recommended; since the quantity of anhydrides added into GSO is much lesser at temperatures that occur just the anhydride isomerization (120 and 180 °C). Then, the best incorporation is achieved at 235 °C for 15 min under microwave irradiation. However, after the renewable synthesis, it was not possible to recover the residual ITA anhydride.

Supplementary Information

Supplementary information (Figures S1 to S7 and Table 1) and Videos S1 and S2 are available free of charge at http://jbcs.sbq.org.br.

Author Contributions

Caroline Gaglieri was responsible for conceptualization, data curation, formal analysis, investigation, validation, visualization, writing original draft, writing-review and editing; Rafael T. Alarcon for formal analysis, investigation, writing original draft, writing-review and editing; Aniele de Moura for formal analysis, investigation, writing original draft, writing-review and editing; Raquel Magri for investigation, visualization, writing original draft; Daniel Rinaldo for software, visualization, writing-review and editing; Gilbert Bannach for conceptualization, funding acquisition, project administration, resources, writing-review and editing.

References

1. Robert, T.; Friebel, S.; *Green Chem.* **2016**, *18*, 2922. [Crossref]
2. Romão, D. C. F.; Santana Jr., C. S.; Brito, M. R.; Scapin, E.; Pedroza, M.; Rambo, M. C. D.; Rambo, M. K. D.; *J. Braz. Chem. Soc.* **2022**, *33*, 938. [Crossref]
3. Gomes, G. R.; Mattioli, R. R.; Pastre, J. C.; *J. Braz. Chem. Soc.* **2022**, *33*, 815. [Crossref]
4. de Albuquerque, D. Y.; Teixeira, W. K. O.; Narayanaperumal, S.; Schwab, R. S.; *J. Braz. Chem. Soc.* **2022**, *33*, 637. [Crossref]
5. Spanedda, M. V.; Bourel-Bonnet, L.; *Bioconjugate Chem.* **2021**, *32*, 482. [Crossref]
6. Gopaliya, D.; Kumar, V.; Khare, S. K.; *Biocatal. Agric. Biotechnol.* **2021**, *36*, 102130. [Crossref]
7. Kuenz, A.; Krull, S.; *Appl. Microbiol. Biotechnol.* **2018**, *102*, 3901. [Crossref]
8. Fraga, G. V.; Ruy, A. D. S.; Pontes, L. A. M.; Campos, L. M. A.; Teixeira, L. S. G.; *Quim. Nova* **2020**, *43*, 951. [Crossref]
9. Teleky, B.-E.; Vodnar, D. C.; *Polymers* **2021**, *13*, 3574. [Crossref]
10. Nayak, P. S.; Narayana, B.; Sarojini, B. K.; Sheik, S.; Shashidhara, K. S.; Chandrashekar, K. R.; *J. Taibah Univ. Sci.* **2016,** *10*, 823. [Crossref]
11. Aldalbahi, A.; Rahaman, M.; El-Faham, A.; *Int. J. Polym. Sci.* **2020**, *67*, 213. [Crossref]
12. Kučera, F.; Petruš, J.; Matláková, J.; Jančář, J.; *React. Funct. Polym.* **2017**, *116*, 49. [Crossref]

13. Petruš, J.; Kučera, F.; Petruj, J.; *Eur. Polym. J.* **2016**, *77*, 16. [Crossref]

14. Kashyap, P. K.; Negi, Y. S.; Goel, N. K.; Diwan, R. K.; Rattan, S.; *Radiat. Phys. Chem.* **2022**, *198*, 110243. [Crossref]

15. Chiriac, A. P.; Nita, L. E.; Diaconu, A.; Bercea, M.; Tudorachi, N.; Pamfil, D.; Mititelu-Tartau, L.; *Int. J. Biol. Macromol.* **2017**, *98*, 407. [Crossref]

16. Lai, H.; Liu, S.; Yan, J.; Xing, F.; Xiao, P.; *Chem. Eng.* **2020**, *8*, 4941. [Crossref]

17. Rengganis, D.; Rachmawati, R.; *Key Eng. Mater.* **2021**, *874*, 149. [Crossref]

18. Shan, Y.; Liu, T.; Zhao, B.; Hao, C.; Zhang, S.; Li, Y.; Wu, Y.; Zhang, J.; *Chem. Eng. J.* **2020**, *385*, 123960. [Crossref]

19. Bai, Y.; Clark, J. H.; Farmer, T. J.; Ingram, I. D. V.; North, M.; *Polym. Chem.* **2017**, *8*, 3074. [Crossref]

20. Gaglieri, C.; Alarcon, R. T.; de Moura, A.; Magri, R.; da Silva-Filho, L. C.; Bannach, G.; *J. Braz. Chem. Soc.* **2021**, *32*, 2120. [Crossref]

21. Alarcon, R. T.; Gaglieri, C.; de Souza, O. A.; Rinaldo, D.; Bannach, G.; *J. Polym. Environ.* **2020**, *28*, 1265. [Crossref]

22. Farmer, T. J.; Macquire, D. J.; Comeford, J. W.; Pellis, A.; Clark, J. H.; *J. Polym. Sci., Part A: Polym. Chem.* **2018**, *56*, 1935. [Crossref]

23. Galanti, M. C.; Galanti, A. V.; *J. Org. Chem.* **1982**, *47*, 1572. [Crossref]

24. Marsilla, K. I. K.; Verbeek, C. J. R.; *Eur. Polym. J.* **2015**, *67*, 213. [Crossref]

25. Okuda, T.; Ishimoto, K.; Ohara, H.; Kobayashi, S.; *Macromolecules* **2012**, *45*, 4166. [Crossref]

26. Aoki, S.; Fukui, A.; *Polym. J.* **1998**, *30*, 295. [Crossref]

27. Mundo dos óleos, https://www.mundodosoleos.com/products/oleo-de-semente-de-uva?variant=31299869048950, accessed in September 2022.

28. Gaglieri, C.; de Moura, A.; Alarcon, R. T.; Magri, R.; Bannach, G.; *J. Therm. Anal. Calorim.* **2022**, *147*, 9095. [Crossref]

29. Lee, J.-S.; Yoon, N.-R.; Kang, B.-H.; Lee, S.-W.; Gopalan, S.-A.; Jeong, H.-M.; Lee, S.-H.; Kwon, D.-H.; Kang, S.-W.; *Sensors* **2014**, *14*, 11659. [Crossref]

30. Malik, P. K.; Tripathy, M.; Patel, S.; *ChemistrySelect* **2020**, *5*, 3551. [Crossref]

31. Bae, J.-S.; Son, Y.-A.; Kim, S.-H.; *Fibers Polym.* **2008**, *9*, 659. [Crossref]

32. Nigam, S.; Rutan, S.; *Appl. Spectrosc.* **2001**, *55*, 362A. [Crossref]

33. Umadevi, M.; Vanelle, P.; Terme, T.; Rajkumar, B. J. M.; Ramakrishnan, V.; *J. Fluoresc.* **2008**, *18*, 1139. [Crossref]

34. Atkins, P.; Overton, T.; Rourke, J.; Weller, M.; Armstrong, F.; Hagerman, M.; *Shriver & Atkins' Inorganic Chemistry*; 5th ed.; W. H. Freeman and Company: New York, USA, 2010.

35. Schneider, K. J.; Williams, J. D.; *Curr. Org. Chem.* **2011**, *15*, 2893. [Crossref]

36. Cottet, C.; Salvay, A. G.; Peltzer, M. A.; Fernández-García, M.; *Polymers* **2021**, *13*, 200. [Crossref]

37. Alarcon, R. T.; Gaglieri, C.; Caires, F. J.; Magdalena, A. G.; de Castro, R. A. E.; Bannach, G.; *Food Chem.* **2017**, *237*, 1149. [Crossref]

38. Gálico, D. A.; Perpétuo, G. L.; Castro, R. A. E.; Treu-Filho, O.; Legendre, A. O.; Galhiane, M. S.; Bannach, G.; *J. Therm. Anal. Calorim.* **2014**, *115*, 2385. [Crossref]